





# Wave propagation and band tails of two-dimensional disordered systems in the thermodynamic limit

Michael A. Klatt<sup>a,b,1</sup> , Paul J. Steinhardt<sup>c,1</sup> , and Salvatore Torquato<sup>c,d,1</sup>

Edited by Georg Maret, Universität Konstanz, Konstanz, Germany; received August 8, 2022; accepted November 6, 2022 by Editorial Board Member Paul Chaikin

Understanding the nature and formation of band gaps associated with the propagation of electromagnetic, electronic, or elastic waves in disordered materials as a function of system size presents fundamental and technological challenges. In particular, a basic question is whether band gaps in disordered systems exist in the thermodynamic limit. To explore this issue, we use a two-stage ensemble approach to study the formation of complete photonic band gaps (PBGs) for a sequence of increasingly large systems spanning a broad range of two-dimensional photonic network solids with varying degrees of local and global order, including hyperuniform and nonhyperuniform types. We discover that the gap in the density of states exhibits exponential tails and the apparent PBGs rapidly close as the system size increases for nearly all disordered networks considered. The only exceptions are sufficiently stealthy hyperuniform cases for which the band gaps remain open and the band tails exhibit a desirable power-law scaling reminiscent of the PBG behavior of photonic crystals in the thermodynamic limit.

photonic band gaps | correlated disorder | hyperuniformity | stealthy | finite-size effects

Band gaps and band tails are well-known features observed in the electric, photonic, phononic, and elastic band structures of ordered materials (1, 2) that play a critical role in applications. For certain crystals, the formation of band gaps in the limit of infinite system size (*thermodynamic limit*) is well established (1, 3). There is also strong evidence for the existence of band gaps in certain quasicrystals (2, 4, 5).

In this paper, we consider a broad range of two-dimensional (2D) isotropic networks with different degrees of correlated disorder and study how their photonic band gap (PBG) and band tail properties depend on system size. Many past numerical studies of PBGs in disordered heterostructures have been based on relatively small systems sizes, such as networks of a few hundred vertices (6–12). Our goal, both as a matter of fundamental physics and for the purpose of practical applications, is to determine whether the conclusions based on these smaller disordered systems persist as the system size gets larger, even approaching the thermodynamic limit.

In particular, we explore the conjecture that stealthy hyperuniformity with sufficiently high  $\chi$  values is a necessary condition for PBGs to persist in isotropic disordered networks in the thermodynamic limit; see ref. 13 and references therein. The vertices in a 2D isotropic disordered network are hyperuniform if  $N(R)$ , the number of vertices within a circular window of radius  $R$ , has a number variance  $\sigma_N^2(R)$  that grows more slowly than  $R^2$  as  $R \rightarrow \infty$  (13, 14); or equivalently, the scattering intensity  $S(k)$  approaches zero for wavenumbers  $k \rightarrow 0$ . Stealthy hyperuniform patterns are ones in which  $S(k) = 0$  for a range of wavenumbers  $0 < k < K$ , as in the case for crystals (15).

Disordered stealthy hyperuniform samples can be constructed via the collective-coordinate optimization technique (16, 17) as ground states of a potential that effectively constrains  $S(k)$  for a prescribed range of wave vectors. For stealthy hyperuniform patterns, the constraint sets  $S(k) = 0$  for  $0 < k < K$ , though other options will also be considered below. The degree of stealthiness is measured by the parameter  $\chi$ , which is proportional to the ratio of the reciprocal space volume of wave vectors with constrained values to the total number of degrees of freedom; specifically, for 2D networks,  $\chi = K^2/(16\pi\rho)$ , where  $\rho$  is the number density (15).

Isotropic disordered patterns are possible only for  $\chi < 1/2$ . The conjecture is that, for fixed dielectric contrast and structural parameters (such as the radius of the disks located at the vertices and the thickness of the network walls), complete PBGs in isotropic disordered networks can persist only for stealthy hyperuniform patterns and only for some limited range of  $\chi$ ,  $\chi_{\text{crit}} \leq \chi < 1/2$ , which is what is meant by “sufficiently large  $\chi$ ”

## Significance

For many years, physicists and material scientists have explored the possibility that there exist disordered systems with (electronic, phononic, photonic) band gaps. Whether these gaps persist as the system size increases is a problem of great fundamental interest, and its answer is desirable for many applications. In this paper, we focus on the case of photonics and show that numerical results based on single modest-sized examples are inadequate to decide the issue. Using the computationally intensive two-stage ensemble method described in this paper, we find that three key structural properties are necessary for complete photonic band gaps to persist in the thermodynamic limit, where only a special subset of disordered systems, known as “highly stealthy hyperuniform,” possess these properties.

Author contributions: M.A.K., P.J.S., and S.T. designed research; M.A.K., P.J.S., and S.T. performed research; M.A.K., P.J.S., and S.T. analyzed data; and M.A.K., P.J.S., and S.T. wrote the paper.

The authors declare no competing interest.

This article is a PNAS Direct Submission. G.M. is a guest editor invited by the Editorial Board.

Copyright © 2022 the Author(s). Published by PNAS. This article is distributed under [Creative Commons Attribution-NonCommercial-NoDerivatives License 4.0 \(CC BY-NC-ND\)](https://creativecommons.org/licenses/by-nc-nd/4.0/).

<sup>1</sup>To whom correspondence may be addressed. Email: klattm@hhu.de, steinh@princeton.edu, or torquato@princeton.edu.

This article contains supporting information online at <http://www.pnas.org/lookup/suppl/doi:10.1073/pnas.2213633119/-/DCSupplemental>.

Published December 20, 2022.

in the conjecture. If for an isotropic disordered pattern, there is no  $\chi_{\text{crit}} < 1/2$ , then no PBG persists for the given dielectric and structural parameters.

The conjecture is based on the finding that stealthy hyperuniformity with sufficiently high  $\chi$  values automatically combines several closely related properties analogous to crystals while still being isotropic: *i*) no single scattering from intermediate to infinite wavelengths; *ii*) holes are strictly bounded with maximal size on the order of the mean nearest neighbor distance (18, 19); and *iii*) a high degree of short-range order as  $\chi$  becomes large (15–17). Each of these attributes due to high  $\chi$  values avoids an effect that can close an apparent PBG in the thermodynamic limit.

Aside from these properties (*i*)–(*iii*), another condition that favors complete PBGs in two dimensions is uniform local topology such that a network consists entirely of trivalent vertices (6). In this paper, we impose this property using the Delaunay-centroidal mapping technique introduced in ref. 6. The technique transforms a stealthy hyperuniform pattern of points into a trivalent network that shares properties (*ii*) and (*iii*) above but which is not precisely stealthy. The deviation from strict stealthiness produced by the mapping appears to be negligible within our numerical accuracy, but we comment further in the conclusions.

Notably, numerical calculations of the band structure for many different types of isotropic disordered networks that are not hyperuniform or not stealthy or do not have large  $\chi$  indicate complete PBGs, in apparent contradiction to the conjecture. However, the calculations are limited to relatively small networks or periodic approximants with relatively few vertices per unit cell, which cannot technically be regarded as truly isotropic disordered systems. The latter is defined only in the thermodynamic limit. To test whether the PBGs remain open for networks required for larger-scale practical applications and in the thermodynamic limit, the commonly used approach of computing the band structure for single instances is not sufficient since existing highly accurate algorithms, such as the plane wave expansion method (20) used in our study, can be applied only to modest-sized networks consisting of several thousand vertices. To extend our reach, we apply a two-stage density of states (DoS) ensemble method that approximates the behavior for larger systems by stacking the DoSs for a large ensemble of modest-sized individual members checking for convergence as the number of members in the ensemble is increased. The DoS ensemble approach not only makes it possible to determine whether apparent PBGs close or remain open as the system size increases but also enables the investigation of the band tail shapes with unprecedented precision.

To achieve this precision, we undertook a substantial computational effort as required to check the conjecture. Analyses of some of the systems required a computation time equivalent to about 200 years on a single 2.4 GHz Skylake processor. The total computation time for the results presented here is about 500 y.

We apply the DoS ensemble method to a spectrum of disordered networks satisfying different combinations of the properties deemed essential by the conjecture—bounded holes, hyperuniformity, and a high degree of stealthiness—as summarized in Table 1 near the end of the paper. Examples include networks with one, two, all three, or none of the properties.

Although each example appears to produce “apparent” complete PBGs based on numerical results obtained for small system sizes, only those possessing all three properties maintain complete PBGs for larger system sizes. Furthermore, the DoS ensemble method shows that systems that do not possess all three properties have exponential band tails of the “apparent” PBG that overlap

at some finite DoS, rapidly closing the supposed gap or, at best, leading to a deep pseudogap. By contrast, to within the numerical and statistical accuracy achievable, the PBGs remain open for networks satisfying all three properties; and band tails exhibit a power-law scaling reminiscent of the tails in crystal systems in which the band gap is known to remain open.

## 1. Network Models

We generate a broad spectrum of models with correlated disorder that encompasses nonhyperuniform and hyperuniform states with varying degrees of long-range order. The resulting models possess different combinations of the three properties (hyperuniformity, stealthiness with high  $\chi$ , bounded holes) conjectured to be essential for PBGs in the thermodynamic limit.

We rely heavily on the powerful collective-coordinate optimization technique (15–17), which is a reciprocal-space-based approach that generates patterns with targeted structure factors by defining a suitable potential that constrains, at the ground state, the values of  $S(k)$  for a prescribed range of wave vectors. The other wave vectors are left free to be set by the optimization. By tailoring the structure factor, this procedure enables us to design a variety of both hyperuniform and nonhyperuniform states. The different models below correspond to different constraints on  $S(k)$ . On the other hand, the nonhyperuniform random sequential addition (RSA) does not require the collective coordinate technique as described below. In all of our models, we choose the unit of length so that we compare the resulting samples at unit number density. We, moreover, compare samples with the same constant number of points per sample.

After constructing the point patterns, we convert them into trivalent networks using the Delaunay-centroidal method from ref. 6, since this uniform local topology is known to be favorable for complete PBGs in two dimensions. Therefore, we first construct the Delaunay triangulation and then connect the centroids of neighboring cells. This choice of connecting the centers of mass (instead of the centers of circumference as in the standard Voronoi tessellation) reduces the variations in bond length and angles. Importantly, the Delaunay-centroidal method preserves the bounded hole property as we rigorously prove in *SI Appendix*. Finally, we decorate the nodes of the network with discs and the edges with walls of finite thickness and adjust the disc radii (0.16) and wall thicknesses (0.08) to facilitate the formation of complete PBGs (6). For comparison, we use a dielectric contrast of 13 as commonly used in earlier studies (1). Our previous studies of gap dependence on dielectric contrast, e.g. ref. 21, suggest that, beyond a contrast of about 10, the qualitative behavior does not depend sensitively on this choice.

**Stealthy Hyperuniform.** Stealthy hyperuniform systems can be found as highly degenerate ground states of a class of bounded pair potentials with compact support in Fourier space (15). Using the collective-coordinate procedure, as explained above, we here simulate stealthy hyperuniform samples by a quench from high temperatures to a disordered ground state (15–17). For  $\chi < 0.5$ , these stealthy ground states are fully disordered and isotropic; at  $\chi = 0.5$ , there is a phase transition from disordered to ordered ground states (15, 22). We simulate samples at two different  $\chi$  values: an intermediate value,  $\chi = 0.25$ , as well as a high value,  $\chi = 0.48$ , to determine when  $\chi$  is sufficiently high, as proposed by the conjecture. At unit number density,  $\chi = 0.48$  corresponds to  $K = 4.9$ . We ensure the fidelity of our stealthy hyperuniform samples by checking that the collective coordinate

optimization is run until the energy above the ground state is less than  $10^{-19}$  times what it was for the random (Poisson) initial state.

**Perfect Glass.** To test the conjecture for a system that is hyperuniform but not stealthy, we simulate samples with a power-law scaling  $S(k) = 0.02 k^2$  for  $k < K = 7.5$  around the origin (which corresponds to  $\chi = 1.11$ ) using the collective-coordinate procedure. This system is called a perfect glass because the ground state manifold contains no crystalline phase (23).

**Stealthy Nonhyperuniform.** Next, we want to check whether it is sufficient if the system is stealthy for a range of finite wavelengths (but not hyperuniform, which would require a range from finite to infinite wavelengths). The target structure factor is one for  $k < K_1$  and zero for  $K_1 < k < K_2$ . Here, we take  $K_1 = 0.5$  and  $K_2 = 4.9$  (i.e., the structure factor vanishes for wavelengths in the range from about 1.3 to 13). The  $\chi$  value is, therefore, again 0.48. To increase the short-range order and to obtain a minimal distance between the points, we add a soft-core repulsion to the long-range potential of the collective-coordinate procedure. More specifically, we employ the same simulation procedure as in ref. 24.

**Equiluminous.** An equiluminous point pattern is one in which the scattering intensity or structure factor is constant for a range of wave vectors (17). Here, we take  $S(k)$  to be the positive constant of  $10^{-2}$  for  $k < K = 4.9$ , indicating that it is neither hyperuniform nor stealthy. It also lacks the bounded hole size. Thus, we test the conjecture with a system whose local structure is quantifiably similar to a stealthy hyperuniform system with  $\chi = 0.48$  but with none of the three properties deemed essential according to the conjecture. To simulate the samples, we use the same procedure as for the perfect glass.

**RSA.** Random sequential addition/adsorption (RSA) is a classic model of nonoverlapping disks that are randomly placed in the system, one after the other (25, 26). The packing fraction  $\phi$  is the fraction of area covered by the disks. At saturation, i.e., at the maximal possible volume fraction  $\phi = 0.5470735$  (28) (27), no further disk can be inserted into the system. We simulate RSA samples at  $\phi = 0.547$  using the simulation procedure from ref. 27.

Among all of the models, the ones that satisfy the bounded hole property are *i*) stealthy hyperuniform states, as explained in the *Introduction* (18, 19), *ii*) the perfect glass, as recently shown (28), and *iii*) RSA at saturation, where by construction, the remaining holes are smaller than the size of an RSA disk. The perfect glass is hyperuniform but not stealthy, and RSA disks are neither stealthy nor hyperuniform (27, 29). For the stealthy nonhyperuniform and equiluminous systems, we observe exponential tails in the distribution of hole sizes, which indicates unbounded holes.

## 2. DoS Ensemble Method

To reliably capture rare events that determine the tail behavior of the PBGs, we use the plane-wave expansion method (20). In contrast, finite-difference time-domain (FDTD) methods allow for larger system sizes but at the expense of accuracy. They may miss eigenfrequencies or locate spurious ones (1).

Such precise results can currently only be obtained for networks with up to about 10,000 vertices. To approximate the behavior for larger systems, we use a two-stage DoS ensemble

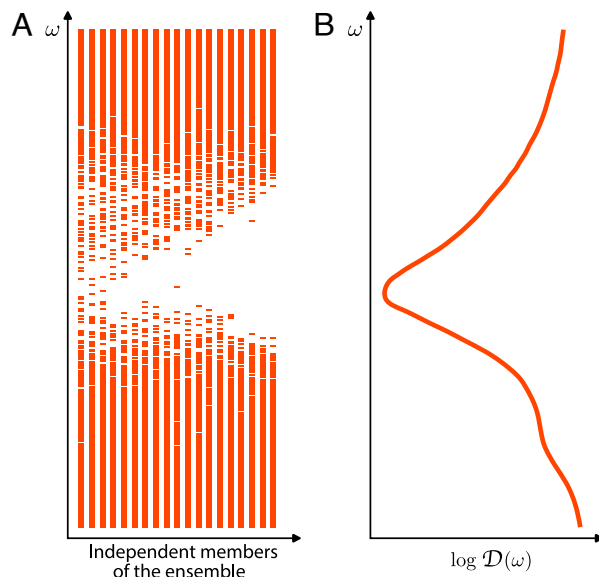


**Fig. 1.** Schematic of our two-stage DoS ensemble method: (A) Band structures for different members of the ensemble are placed side-by-side and ordered by gap sizes, increasing from left to right in panel (A); (B) The DoS  $\mathcal{D}(\omega)$  is averaged over all members of the ensemble.

method (Fig. 1). First, we compute the band structures for a large ensemble of modest-sized members of the ensemble. The area-normalized DoS  $\mathcal{D}(\omega)$  is then defined as

$$\mathcal{D}(\omega) := \frac{1}{A} \sum_{i=1}^{\infty} \delta(\omega - \omega_i), \quad [1]$$

where  $A$  is the total area of the sample and the  $\omega_i$  are the frequencies of the eigenmodes (at the  $\Gamma$  point). Note that because of the isotropy, a single Bloch wavevector suffices. The area-normalized DoS has dimensions  $1/(\text{frequency} \times \text{area})$ . Here the units of length and time are set by our choice of  $c = 1$  for the speed of light and  $\rho = 1$ , i.e., a unit number density. For our finite samples, we approximate the DoS (defined by Dirac delta distributions  $\delta$ ) by a corresponding histogram. In the next step, we average the DoS for the entire ensemble checking for convergence as the number of members in the ensemble is increased. Finally, we compare the average DoS for increasingly large system sizes, i.e., number of vertices per sample (ranging over about two orders of magnitude). The DoS converges within our statistical and systematic uncertainty. This is consistent with our underlying assumption of ergodicity.

Fig. 1 is a schematic that illustrates our two-stage DoS ensemble method based on two different ways of representing the nature of the photonic states. The left-hand side schematically shows the computed band structure for different members of the ensemble placed side by side ordered from the smallest to the largest gap, going left to right. Even though individual members of the ensemble may appear to exhibit a PBG, one can see by eye whether the band gaps of different members of the ensemble are sufficiently offset with respect to each other so that no common PBG remains. This behavior is expected if there is no surviving PBG in the large system limit. If, instead, the PBG remains in the band structures for all members of the ensemble when they are placed side by side, the PBG may remain open in the large system limit. The right-hand side of Fig. 1 schematically depicts the DoS  $\mathcal{D}(\omega)$  averaged over all members of the ensemble. (See Fig. S5

in ref. 30 for an example obtained for TM polarization only that shows variations of the PBG between different realizations based on 500 samples of disk packings each containing 200 disks.)

For our studies of complete band gaps (both TM and TE polarizations and in all directions), we find that a system size of about 400 vertices is required to reach the point where there is only weak dependence of  $\mathcal{D}(\omega)$  on the sample size. To determine  $\mathcal{D}(\omega)$  for larger sizes with the requisite accuracy, we introduce an ensemble of many samples with the largest accessible single-sample size (up to 9,600 vertices per sample), where the number of members of the ensemble varies from about 50 to 500,000 depending on the single-sample size. With this DoS ensemble approach, we are able to study not just the PBGs but also the band tails, from which we can infer whether they close in the thermodynamic limit.

### 3. Results

The band tail behavior is essential for determining whether a PBG can persist in the thermodynamic limit in a strict sense, i.e., whether the DoS can vanish, at least in principle, exactly over some finite range of frequencies as the volume goes to infinity. If either the upper or lower band tails (or both) have an exponential form, the tails must cross (closing the apparent PBG) at a finite DoS  $\mathcal{D}_{\min}$ . In contrast, power-law tails may be sufficiently separated in frequency such that there remains a finite range of frequencies between the tails for which the DoS is strictly zero even in the limit of infinite system size, i.e., the PBG may remain open in the thermodynamic limit.

Of course, we cannot rigorously prove the asymptotic tail behavior since, numerically, we can only probe finite system sizes. However, the outcome of our DoS ensemble approach, which entails sufficiently intensive computational effort to perform the strong convergence tests described in *DoS Ensemble Method*, is strongly suggestive.

For an exponential tail of the DoS  $\mathcal{D}(\omega)$ , there is no strict band edge. Here, we look for exponential-tail behaviors described by

$$\mathcal{D}(\omega) \sim \exp(\pm\beta_{\pm}\omega), \quad [2]$$

with constants  $\beta_{\pm} > 0$ ; Fig. 2A.

A power-law tail of  $\mathcal{D}(\omega)$  is defined in reference to a well-defined edge frequency  $\omega_0$ :

$$\mathcal{D}(\omega) \sim |\Delta\omega|^{\gamma}, \quad [3]$$

where  $\Delta\omega := \omega - \omega_0$  and  $\omega_0$  is the limiting value where the band tail vanishes, i.e.,  $\mathcal{D}(\omega) \rightarrow 0$  for  $\omega \rightarrow \omega_0$ ; we use the subscript and superscript  $\pm$  on the quantities  $\gamma_{\pm}$  and  $\omega_0^{\pm}$  to refer to the upper and lower tails, respectively; Fig. 2B.

Table 1 provides a synopsis of our results for all isotropic disordered models considered; specifically, those that exhibit exponential versus power-law tails in the DoS for TE and TM polarizations, respectively, and, hence, those that potentially possess complete PBGs in the thermodynamic limit. The table also includes the particular parameters and attributes, including whether the model is hyperuniform, whether it is stealthy and whether it has bounded holes, i.e., the three attributes that

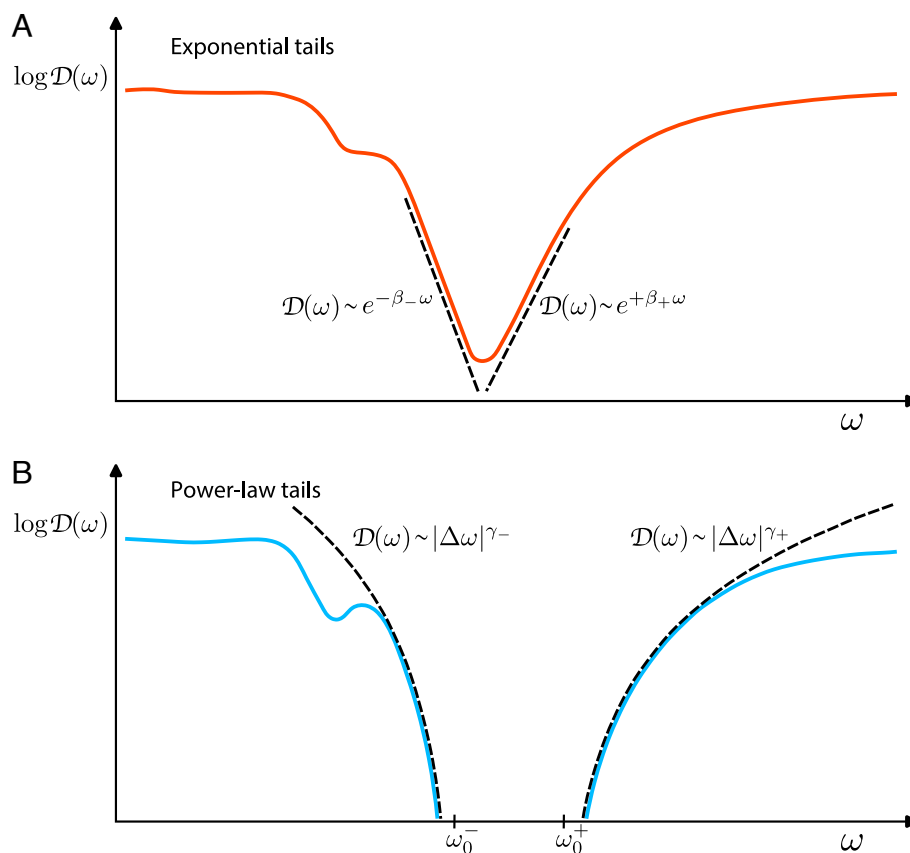


**Fig. 2.** Schematic of exponential and power-law tail behaviors: (A) The typical behavior that we observe for most disordered systems is exponential, which inevitably leads to a closing of the apparent PBG in the infinite system size limit. (B) Power-law tails are an atypical behavior, for which the DoS can be strictly zero for a range of frequencies even in the limit of infinite system size if the power-law tails are sufficiently separated in frequency. The subscript and superscript  $\pm$  on the quantities  $\beta_{\pm}$ ,  $\omega_0^{\pm}$ , and  $\gamma_{\pm}$  refer to the upper and lower tails, respectively.



**Table 1. Overview of the structural and photonic properties of our models**

System labels		Hyper-uniform	Stealthy	Bounded holes	TE	TM	PBGs persists
Stealthy hyperuniform	$\chi = 0.48$	✓	✓	✓	PL	PL	✓
	$\chi = 0.25$	✓	✓	✓	CC	CC	✗
Perfect glass	$\chi = 1.11$	✓	✗	✓	CC	Exp	✗
Stealthy nonhyperuniform	$\chi = 0.48$	✗	✓	✗	Exp	CC	✗
Equiluminous ( $10^{-2}$ )	$\chi = 0.48$	✗	✗	✗	Exp	Exp	✗
RSA	$\phi = 0.55$	✗	✗	✓	Exp	Exp	✗

The labels of the systems refer to the specific models defined in *Network Models*, where their parameters and properties are explained in detail. The tails of the apparent PBGs are classified as “Exp,” which means that one or both band tails fit an exponential form (consistent with a closing of the apparent PBG at large system sizes) or “PL,” which means that both band tails are consistent with a power-law decay. If the tails meet at a too high DoS ( $\mathcal{D}_{\min} \gtrsim 0.1$ ), which does not allow for identification of the tail behavior, we classify the tails as crisscross “CC” (i.e., the apparent PBG closes rapidly as the system size increases). The last column indicates systems for which the DoS exhibits a PBG for the largest systems in our study and potentially in the thermodynamic limit; these results are consistent with the band tail behavior reported in the previous two columns.

arise from the conjectured necessary properties for PBGs in the thermodynamic limit, as discussed in the *Introduction*.

Each of our models has a sufficient degree of short-range order that small samples with a few hundred vertices per unit cell exhibit seemingly substantial PBGs. For example, for an RSA network with 200 vertices, we find a gap-to-midgap ratio of about 20% and 11% for TE and TM polarization respectively. However, as the system size increases, the supposed PBGs quickly diminish. A similar effect can be observed in our DoS ensemble approach. Assuming ergodicity, we construct ensembles of finite samples. Even if every individual finite network in the ensemble has an apparent complete PBG, the frequencies vary between samples, similar to what is illustrated in Fig. 1. When the band structures are stacked, the apparent PBG closes as the number of independent ensemble members increases—in fact, it closes at a finite resolvable DoS. For example, for our RSA networks, both the TE and TM pseudogaps bottom out at  $\mathcal{D}_{\min} \approx 10^{-3}$ . Hence, our ensemble method shows that both the apparent TE and TM PBGs for RSA networks do not survive in the large system size limit.

For all models, except the disordered stealthy hyperuniform one with a high  $\chi$  value of 0.48, we observe a similar closing of both the apparent TE and TM PBGs, despite the fact that their PBGs appear to be open based on studies of smaller samples—see the last column of Table 1, Fig. 3, and *SI Appendix*, Fig. S1. The closing of the supposed PBGs includes systems that are hyperuniform but nonstealthy as well as stealthy nonhyperuniform examples (see columns 2 and 3). In all of these systems, even the apparent TM PBGs close, which are often considered to be more easily created than TE PBGs. In all cases, the tails are consistent with exponential decay (see columns 5 to 8), except in cases (marked CC in the table) where the tails crisscross and close the supposed PBG at such high DoS that the tail is too short to determine the asymptotic behavior.

For the stealthy hyperuniform networks with  $\chi = 0.48$ , both the TE and TM PBGs remain open for the largest systems in our study and potentially in the thermodynamic limit since the tails are consistent with a power law behavior; see Figs. 3 and 4. Stealthy hyperuniformity with a high  $\chi$  value is the only candidate remaining, to the extent to which we can determine, for a complete PBG in the thermodynamic limit.

An important subtlety is that the networks labeled “stealthy” in Table 1 are not precisely stealthy because conversion via the Delaunay-centroidal method to a trivalent network introduces small deviations from perfect stealthiness (i.e.,  $S(k)$  is not precisely zero for  $0 < k < K$  as it is for the point pattern). According to the conjecture, we should expect a transition

“deep down the tail” to an exponential-tail behavior like for the equiluminous system. For example, if we check the TM behavior of disk packings, where the disks are set on the original point

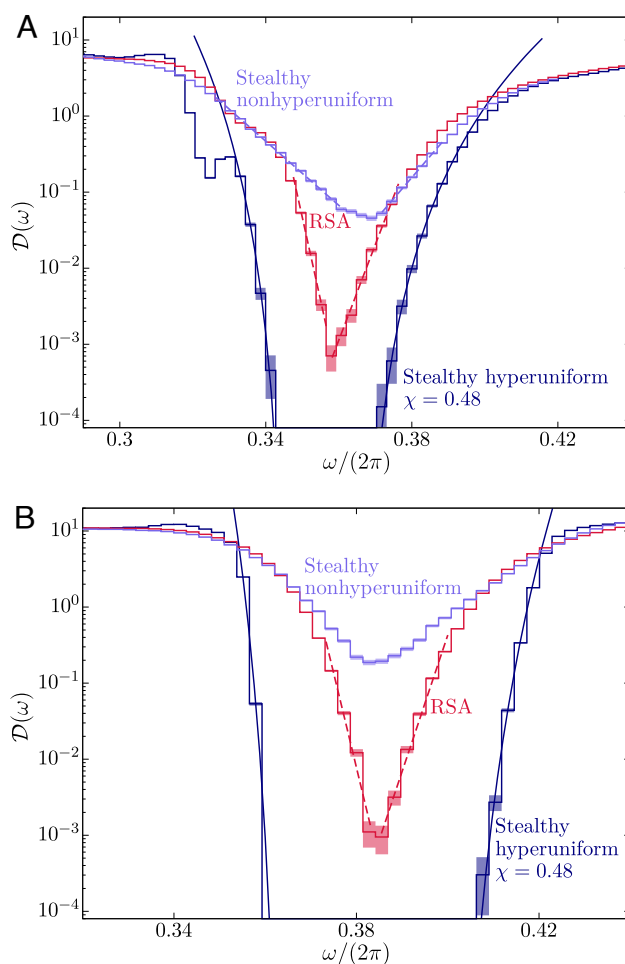


**Fig. 3.** Average DoS  $\mathcal{D}(\omega)$  for (A) TE and (B) TM polarization. The vertical color bands indicate the standard error. For both the stealthy nonhyperuniform and RSA model, the tails cross and close the apparent PBG; in the former case, the tails crisscross, and in the latter case, the tails are consistent with an exponential decay (dashed lines), which inevitably leads to a closing of the supposed PBG (Fig. 2A). In contrast, for the stealthy hyperuniform model with  $\chi = 0.48$ , both the TE and TM PBGs remain open for the largest systems in our study, and the tails are consistent with a power-law behavior (solid lines); see Fig. 4 for a log-log plot. This scaling allows the PBGs to remain open even in the thermodynamic limit if the tails are sufficiently separated in frequency; Fig. 2B.

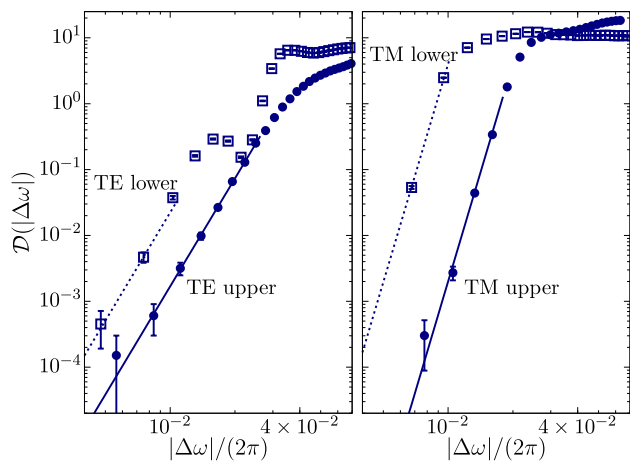


**Fig. 4.** Log-log plots of the tail behavior for the stealthy hyperuniform model with  $\chi = 0.48$  for (Left) TE and (Right) TM polarization. For the upper tails, a power-law scaling is observed over several orders of magnitude of  $\mathcal{D}(\omega)$ . The lower tails are too steep to resolve the scaling, but their behavior is consistent with a power law with the same exponent as for the corresponding upper tail.

patterns of equiluminous systems with  $\chi = 0.48$  as in Table 1, we observe a crossover to exponential tails at a DoS below about  $10^{-3}$ , even though  $S(k)$  for  $0 < k < K$  is quite small ( $10^{-2}$ ), implying that the apparent PBG closes; *SI Appendix, Fig. S2*.

Another illuminating comparison is between the TM PBGs of a nonstealthy and nonhyperuniform RSA model (31, 32) composed of disks and a highly stealthy hyperuniform disk packing (24, 30, 33) (again omitting the conversion to a network via the Delaunay-centroidal method). In accordance with the conjecture, we observe exponential tails for the RSA model and a power-law scaling for the stealthy hyperuniform disks model. Although the TM band edges for the RSA disks are substantially apart from one another, the exponential tails indicate that the apparent PBG found in simulations will close at a finite value  $\mathcal{D}_{\min}$ , resulting in a deep pseudogap.

#### 4. Discussion

Our key takeaway from Table 1 is that, except for the disordered stealthy hyperuniform system with  $\chi = 0.48$ , all models considered here have photonic band tails that cross and close the apparent PBG at sufficiently large (but computationally resolvable) system sizes. (In future studies, we will attempt to determine a precise value of  $\chi_{\text{crit}}$ .) Since the exception is the only model that satisfies the three properties—hyperuniform, stealthy with large  $\chi$  [i.e., very near to the maximum value of  $1/2$  in the disordered regime (15)], and bounded holes—the numerical results are consistent with the original conjecture (13) that the three attributes—hyperuniformity, high degree of stealthiness, and bounded holes—are necessary (even if they are not sufficient) for the existence of a PBG in a disordered network in the thermodynamic limit.

We, of course, cannot rigorously prove the conjecture that highly stealthy hyperuniformity is necessary to have complete PBGs based on finite simulations and computation time. However, we have been able to show that a wide range of models that violate the conjecture and that appear to have complete PBGs based on simulations of small systems actually do not maintain complete PBGs as the system size increases.

To be sure, for designers of sufficiently small photonic network solids, the range of disordered structures that have apparent PBGs

is greater. As a matter of principle, though, these apparent PBGs are not inherent features of the type of disordered model (e.g., RSA vs. nonhyperuniform vs. low- $\chi$  stealthy hyperuniform, etc.) but rather strongly depend on the chosen finite system size. Our goal here is to identify disordered structures for which the band gap is inherent, i.e., survives in the thermodynamic limit, as required for a truly disordered system. We recommend our DoS ensemble approach combined with precisely constructed disordered models, high statistics, and convergence tests as useful for testing and assessing robustness of PBGs for general models and sizes.

#### Materials and Methods

**Simulation Details for Network Models.** We start the collective coordinate optimization technique from high-temperature initial conditions, more specifically, the ideal gas in the canonical ensemble. For the optimization of the collective coordinates, we employ a limited-memory Broyden-Fletcher-Goldfarb-Shanno (L-BFGS) optimization algorithm. For the perfect glass, we take  $\gamma = 3$  for the weight function; see Eq. 3 in ref. 23. To compare models with the same number of points per sample, we also condition our simulation of RSA on the number of disks per sample (i.e., we repeat the simulation until the prescribed number of points is obtained).

The number of independent ensemble members ( $M$ ) and the number of vertices per sample ( $V$ ) for which we averaged  $\mathcal{D}(\omega)$  in Fig. 3 are summarized for each polarization ( $P$ ) as a triplet ( $P, M, V$ ), where the number of ensemble members is rounded to the leading digit: stealthy nonhyperuniform (TE,  $10^3, 2,400$ ) and (TM, 200, 2,400); RSA (TE,  $3 \times 10^3, 2,400$ ) and (TM,  $2 \times 10^3, 2,400$ ); and stealthy hyperuniform  $\chi = 0.48$  (TE,  $2 \times 10^3, 2,400$ ) and (TM,  $2 \times 10^3, 2,400$ ). For the other models, *SI Appendix, Fig. S1*.

**Photonic Density of States.** We use the open-source software package MIT Photonic Bands (MPB) (20) to compute the photonic band structures of our disordered networks. By a choice of units, we set the speed of light to  $c = 1$ . We only compute the eigenfrequencies at the  $\Gamma$  point since the models are isotropic. We confirmed the isotropy of the photonic band structure for our finite-sized samples. We set the tolerance of the MPB eigensolver to  $10^{-5}$  and the mesh size for the smoothing of the values of the dielectric constant to five. The resolution parameter was set to 20. The DoS is approximated by a histogram with a fixed bin width of 0.00276.

**Data, Materials, and Software Availability.** The software MPB (20) used in this study is publicly available on the website of the project. The final data of this study will be made available in a Zenodo repository at <https://doi.org/10.5281/zenodo.7315577>.

**ACKNOWLEDGMENTS.** We thank Jaek Kim, Ge Zhang, and Mikael Rechtsman for valuable discussions. The Research was sponsored by the Army Research Office and was accomplished under Cooperative Agreement Number W911NF-22-2-0103. M.A.K. acknowledges funding and support by the Deutsche Forschungsgemeinschaft (DFG, German Research Foundation) through the SPP 2265, under grants numbers ME 1361/16-1, WI 5527/1-1, and LO 418/25-1, as well as by the Volkswagenstiftung via the Experiment Project "Finite Projective Geometry." The simulations presented in this article were substantially performed on computational resources managed and supported by the Princeton Institute for Computational Science and Engineering (PICSciE).

Author affiliations: <sup>a</sup>Institut für Theoretische Physik II: Soft Matter, Heinrich-Heine-Universität Düsseldorf, Düsseldorf 40225, Germany; <sup>b</sup>Experimental Physics, Saarland University, Center for Biophysics, Saarbrücken 66123, Germany; <sup>c</sup>Department of Physics, Princeton University, Princeton, NJ 08544; and <sup>d</sup>Department of Chemistry, Princeton Institute for the Science and Technology of Materials, and Program in Applied and Computational Mathematics, Princeton University, Princeton, NJ 08544

1. J. D. Joannopoulos, S. G. Johnson, J. N. Winn, R. D. Meade, *Photonic Crystals: Molding the Flow of Light* (Princeton University Press, Princeton, ed. 2, 2008).
2. W. Man, M. Megens, P. J. Steinhardt, P. M. Chaikin, Experimental measurement of the photonic properties of icosahedral quasicrystals. *Nature* **436**, 993–996 (2005).
3. P. M. Chaikin, T. C. Lubensky, *Principles of Condensed Matter Physics* (Cambridge University Press, Cambridge, 2000).
4. M. C. Rechtsman, H. C. Jeong, P. M. Chaikin, S. Torquato, P. J. Steinhardt, Optimized structures for photonic quasicrystals. *Phys. Rev. Lett.* **101**, 073902 (2008).
5. M. Florescu, S. Torquato, P. J. Steinhardt, Complete band gaps in two-dimensional photonic quasicrystals. *Phys. Rev. B* **80**, 155112 (2009).
6. M. Florescu, S. Torquato, P. J. Steinhardt, Designer disordered materials with large, complete photonic band gaps. *Proc. Natl. Acad. Sci. U.S.A.* **106**, 20658–20663 (2009).
7. L. S. Froufe-Pérez *et al.*, Role of short-range order and hyperuniformity in the formation of band gaps in disordered photonic materials. *Phys. Rev. Lett.* **117**, 053902 (2016).
8. S. F. Liew *et al.*, Photonic band gaps in three-dimensional network structures with short-range order. *Phys. Rev. A* **84**, 063818 (2011).
9. L. Shi *et al.*, Amorphous photonic crystals with only short-range order. *Adv. Mater.* **25**, 5314–5320 (2013).
10. S. R. Sellers, W. Man, S. Sahba, M. Florescu, Local self-uniformity in photonic networks. *Nat. Commun.* **8**, 14439 (2017).
11. X. Li, A. Das, D. Bi, Biological tissue-inspired tunable photonic fluid. *Proc. Natl. Acad. Sci. U.S.A.* **115**, 6650–6655 (2018).
12. M. I. Tahmid, M. I. Tahmid, D. J. Paul, M. Z. Baten, Emergence and tunability of transmission gap in the strongly disordered regime of a dielectric random scattering medium. *Opt. Express* **29**, 17215–17226 (2021).
13. S. Torquato, Hyperuniform states of matter. *Phys. Rep.* **745**, 1–95 (2018).
14. S. Torquato, F. H. Stillinger, Local density fluctuations, hyperuniformity, and order metrics. *Phys. Rev. E* **68**, 041113 (2003).
15. S. Torquato, G. Zhang, F. H. Stillinger, Ensemble theory for stealthy hyperuniform disordered ground states. *Phys. Rev. X* **5**, 021020 (2015).
16. O. U. Uche, F. H. Stillinger, S. Torquato, Constraints on collective density variables: Two dimensions. *Phys. Rev. E* **70**, 046122 (2004).
17. R. D. Batten, F. H. Stillinger, S. Torquato, Classical disordered ground states: Super-ideal gases and stealth and equi-luminous materials. *J. Appl. Phys.* **104**, 033504 (2008).
18. G. Zhang, F. H. Stillinger, S. Torquato, Can exotic disordered “stealthy” particle configurations tolerate arbitrarily large holes? *Soft Matt.* **13**, 6197 (2017).
19. S. Ghosh, J. L. Lebowitz, Generalized stealthy hyperuniform processes: Maximal rigidity and the bounded holes conjecture. *Commun. Math. Phys.* **363**, 97–110 (2018).
20. S. Johnson, J. Joannopoulos, Block-iterative frequency-domain methods for Maxwell’s equations in a planewave basis. *Opt. Express* **8**, 173 (2001).
21. M. A. Klatt, P. J. Steinhardt, S. Torquato, Gap sensitivity reveals universal behaviors in optimized photonic crystal and disordered networks. *Phys. Rev. Lett.* **127**, 037401 (2021).
22. G. Zhang, F. H. Stillinger, S. Torquato, Ground states of stealthy hyperuniform potentials II. Stacked-slider phases. *Phys. Rev. E* **92**, 022120 (2015).
23. G. Zhang, F. H. Stillinger, S. Torquato, The perfect glass paradigm: Disordered hyperuniform glasses down to absolute zero. *Sci. Rep.* **6**, 36963 (2016).
24. J. Kim, S. Torquato, Multifunctional composites for elastic and electromagnetic wave propagation. *Proc. Natl. Acad. Sci. U.S.A.* **117**, 8764–8774 (2020).
25. S. Torquato, “Random heterogeneous materials” in *Interdisciplinary Applied Mathematics*, S. S. Antman, L. Sirovich, J. E. Marsden, S. Wiggins, Eds. (Springer, New York, ed. 2, 2002), vol. 16.
26. S. N. Chiu, D. Stoyan, W. S. Kendall, J. Mecke, *Stochastic Geometry and Its Applications* (Wiley, Chichester, ed. 3, 2013).
27. G. Zhang, S. Torquato, Precise algorithm to generate random sequential addition of hard hyperspheres at saturation. *Phys. Rev. E* **90**, 053312 (2013).
28. H. Wang, S. Torquato, Equilibrium states corresponding to targeted hyperuniform nonequilibrium pair statistics. arXiv [Preprint] (2022). 10.1039/D2SM01294D. Accessed date 12 October 2022.
29. S. Torquato, H. Wang, Precise determination of pair interactions from pair statistics of many-body systems in and out of equilibrium. *Phys. Rev. E* **106**, 044122 (2022).
30. G. J. Aubry *et al.*, Experimental tuning of transport regimes in hyperuniform disordered photonic materials. *Phys. Rev. Lett.* **125**, 127402 (2020).
31. H. Miyazaki, M. Hase, H. T. Miyazaki, Y. Kurokawa, N. Shinya, Photonic material for designing arbitrarily shaped waveguides in two dimensions. *Phys. Rev. B* **67**, 235109 (2003).
32. C. Rockstuhl, U. Peschel, F. Lederer, Correlation between single-cylinder properties and bandgap formation in photonic structures. *Opt. Lett.* **31**, 1741–1743 (2006).
33. L. S. Froufe-Pérez, M. Engel, J. J. Sáenz, F. Scheffold, Band gap formation and Anderson localization in disordered photonic materials with structural correlations. *Proc. Natl. Acad. Sci. U.S.A.* **114**, 9570–9574 (2017).